International Journal of Heat and Mass Transfer 52 (2009) 4748–4756

Contents lists available at ScienceDirect

International Journal of Heat and Mass Transfer

journal homepage: www.elsevier.com/locate/ijhmt

Experimental and numerical study of convection heat transfer of CO_2 at super-critical pressures during cooling in small vertical tube

Pei-Xue Jiang [a,*], Chen-Ru Zhao [a], Run-Fu Shi [a], Yang Chen [a], Walter Ambrosini [b]

[a] Key Laboratory for Thermal Science and Power Engineering, Department of Thermal Engineering, Tsinghua University, Beijing 100084, China
[b] Department of Mechanical, Nuclear and Production Engineering, University of Pisa, 56126 Pisa, Italy

ARTICLE INFO

Article history:
Received 13 November 2008
Received in revised form 3 June 2009
Accepted 3 June 2009
Available online 21 July 2009

Keywords:
Super-critical pressures CO_2
Cooling condition
Convection heat transfer
Properties variation
Buoyancy

ABSTRACT

Convection heat transfer of CO_2 at super-critical pressures during cooling in a vertical small tube with inner diameter of 2.00 mm was investigated experimentally and numerically. The local heat transfer coefficients were determined through a combination of experimental measurements and numerical simulations. This study investigated the effects of pressure, cooling water mass flow rate, CO_2 mass flow rate, CO_2 inlet temperature, flow direction, properties variation and buoyancy on convection heat transfer in small tube. The results show that the local heat transfer coefficients vary significantly along the tube when the CO_2 bulk temperatures are in the near-critical region. The increase of specific heat and turbulence kinetic energy due to the density variation leads to the increase of the local heat transfer coefficients for upward flow. The buoyancy effect induced by density variation leads to a different variation trend of the local heat transfer coefficients along the tube for upward and downward flows. The numerical simulations were conducted using several k–ε turbulence models including the RNG k–ε model with a two-layer near wall treatment and three low-Reynolds number eddy viscosity turbulence models. The simulations using the low-Reynolds number k–ε model due to Yang–Shih has been found to be able to reproduce the general features exhibited in the experiments, although with a relatively large overestimation of measured wall temperatures. A better understanding of the mechanism of properties variation and buoyancy effects on convection heat transfer of CO_2 at super-critical pressures in a vertical small tube during cooling has been developed based on the information generated by the simulation on the detailed flow and turbulence fields.

1. Introduction

As a natural constituent of the biosphere, CO_2 is a non-flammable, odorless, nontoxic working fluid, with ODP = 0, GWP = 1, and no unexpected long-term effects to the environment. In environmental, cost and safety terms, CO_2 is regarded as an ideal natural refrigerant [1,2]. Thus, the CO_2 high-pressure trans-critical compression cycle for air-conditioners and heat pumps is currently of great interest.

Heat transfer in super-critical fluids is relevant to various engineering applications such as gas cooler in CO_2 trans-critical refrigerating systems, fossil fuel fired steam generators, nuclear reactors, transpiration cooling and convection cooling in rocket thrust chambers, selective extraction in chemical engineering, etc. In the super-critical region, thermophysical properties vary dramatically with a small change in temperature over certain temperature range. Convection heat transfer of fluids at super-critical pressures exhibits many special features due to the sharp variations of the thermophysical properties and buoyancy forces resulting from the non-uniform density distribution across the cross-section of the tube during both heating and cooling process.

In many of these applications mentioned above, the super-critical fluids are used as a coolant for cooling engineering systems, and there have been many research papers published on experimental and numerical studies of internal forced and mixed convection heat transfer of super-critical fluids during heating [3–8]. The results provided significant insight into the special features of heat transfer processes of super-critical pressure fluids during heating. However, in the application of CO_2 trans-critical refrigerating systems, the CO_2 rejects heat in the gas cooler at super-critical pressures. The heat transfer features during this cooling process is different from those during heating. Improved understanding of the convection heat transfer characteristics and the heat transfer enhancement and deterioration mechanisms of CO_2 at super-critical pressures during cooling in small tube is important for improving designs of the compact and high efficiency gas cooler and the internal heat exchanger.

Although applications of CO_2 at super-critical pressures during cooling are not as wide as those during heating, there were still

* Corresponding author. Tel.: +86 10 62772661; fax: +86 10 62770209.
E-mail address: Jiangpx@tsinghua.edu.cn (P.-X. Jiang).

0017-9310/$ - see front matter © 2009 Elsevier Ltd. All rights reserved.
doi:10.1016/j.ijheatmasstransfer.2009.06.014

Nomenclature

C_P	specific heat at constant pressure [J/(kg K)]
d	diameter of small tube [m]
g	gravity acceleration [m^2/s]
G	mass flow rate [kg/s]
H	bulk specific enthalpy [J/kg]
h_x	local heat transfer coefficient [W/(m^2 K)]
k	turbulence kinetic energy [m^2/s^2]
p	pressure [MPa]
Pr	Prantle number
R	inner radius of small tube [m]
r	distance from the axial [m]
Re	Reynolds number
T	temperature [°C]
T_{pc}	pseudo-critical temperature [°C] or [K]
x	axial coordinate [m]
y	normal distance from the inner wall
$y+$	non-dimensional distance from the wall = $\frac{\rho C_\mu^{\frac{1}{4}}\sqrt{k}y}{\mu}$ (C_μ = 0.09)

Greek symbols

δ	tube wall thickness [m]
λ	thermal conductivity of the small tube (stainless seel)
ρ	density of fluid [kg/m^3]
μ	dynamic viscosity [kg/(m s)]

Subscripts

0	tube entrance
CO_2	parameters of CO_2
in	inner surface
out	outer surface
pc	pseudo critical
wall	wall
water	parameters of water

many researches carried out on the convection heat transfer of super-critical fluids in vertical and horizontal normal size tubes during cooling [9–12]. In recent years, the convection heat transfer of fluids at super-critical pressures has also been investigated for mini/micro tubes or channels during cooling prompted by the need for low weight and small volume heat exchangers, such as by Pettersen et al. [13], Liao and Zhao [14], Dang and Hihara [15], Huai et al. [16] and Kuang and Ohadi [17]. Detailed reviews covering the research on heat transfer to fluids at super-critical pressures during cooling were presented by Pitla et al. [18] and Chen et al. [19]. Chen et al. [19] presented a comprehensive analysis of heat transfer and pressure drop experimental data and correlations for super-critical CO_2 cooling in macro- and micro-channels and recommended further efforts be made to develop good heat transfer methods for super-critical CO_2 cooling in the future. Numerical calculations were conducted with various procedures and models to simulate the laminar (Liao and Zhao [20]) or turbulent flow (Petrov and Popov [21], Pitla et al. [22], and Dang and Hihara [23]) and heat transfer of super-critical fluids during cooling. However, most of the previous numerical calculations were conducted without considering the influence of buoyancy effect.

As far as the author concerned, most of the previous studies focused on the axially-averaged heat transfer performance. There is no work experimentally measuring the local convection heat transfer coefficients of super-critical fluids in small tubes during cooling due to the difficulty of the measurements, and there is very few detailed heat transfer mechanism analysis conducted through numerical simulations, especially those related to the influence of properties variation and buoyancy effects. Thus, the purpose of this work was to obtain the local heat transfer coefficients during cooling by a combination of experimental measurements and numerical simulations for the cooling water domain and to investigate the influence of pressure, cooling water mass flow rate, CO_2 mass flow rate, CO_2 inlet temperature, flow direction on heat transfer. Moreover, based on comparisons of measured wall temperatures from the experiments with those obtained from the simulations of the whole domain including the CO_2, tube wall and cooling water regions, appropriate turbulence model was selected to generate detailed information for obtaining an understanding of the influence of the sharp thermophysical properties variations of the fluid and the buoyancy effects.

2. Investigation method

The main difficulty in obtaining the local heat transfer coefficients is to obtain the local heat flux by experimental approach. In order to solve this problem, this investigation combines numerical simulations and experimental measurements to determine the local heat flux. A commercial code FLUENT 6.3 was used to simulate the convection heat transfer of the cooling water in the outside channel to calculate the local outer wall heat flux from the CO_2 to the water through the tube. The local heat transfer coefficients were then obtained using the measured temperature on the outside wall and the local heat fluxes calculated from the numerical simulation.

2.1. Experimental apparatus

The experimental system used to investigate the local convection heat transfer of CO_2 at super-critical pressures in vertical small tube during cooling is shown schematically in Fig. 1. The CO_2 was supplied from the high-pressure CO_2 container, was cooled by the cooling bath and was pressurized by a high-pressure CO_2 pump. A super-critical magnetic pump was used to circulate the fluid in the loop. The mass flow rate of CO_2 was measured using a Coriollis mass flow meter. The CO_2 was heated in a pre-heater before entering the test section, where it was cooled by water running in a Plexiglas channel. Then the CO_2 left the test section and flowed through the sub-cooler where it was cooled. A data acquisition system, standard and differential pressure transducers, thermocouples and RTDs were installed to measure the parameters.

The test section was a 250 mm long vertical tube-in-tube counter-flow heat exchanger, with 150 mm cooling section and 50 mm adiabatic section before and after. The test section was connected with the test loop by flanges and high-pressure fittings. The inner tube was a smooth stainless steel 1Cr18N9T tube with inside and outside diameters of 2.00 mm and 3.14 mm. The test section was heavily insulated and hence the losses to the environment were negligible. Also, the axial conduction in the steel tube and the fluids are found to be insignificant.

Mixers were installed before points where the inlet and outlet CO_2 temperatures were measured by accurate RTDs (Pt-100), which contact the CO_2 through a tee joint. The CO_2 inlet pressure was measured by a pressure transducer. The location for measuring temperature and pressure of test section is shown in Fig. 1. The local outer wall temperatures of the small tube were measured

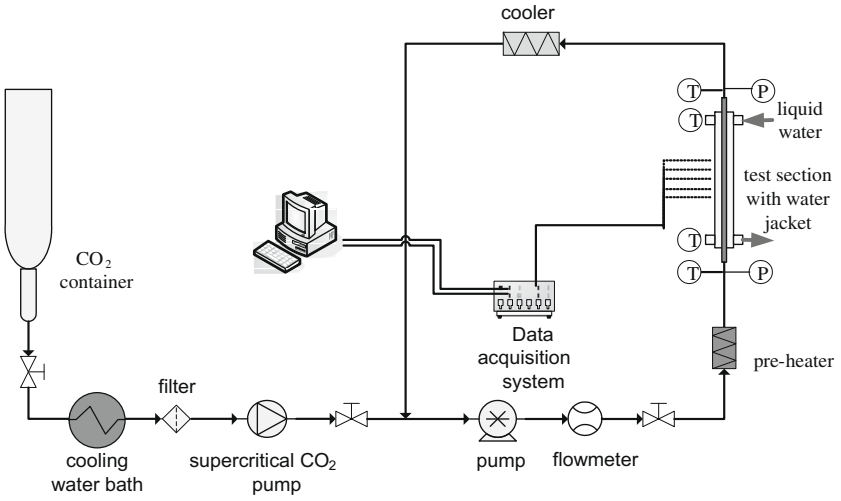

Fig. 1. Schematic of experimental system.

using 10 equally spaced T-type thermocouples welded onto the outer surface of the tube. The inlet and outlet temperatures of the cooling water were measured by sheathed thermocouples. The cooling water mass flow rate was measured using the weighing method.

2.2. Method to evaluate the local heat transfer coefficient

The local heat transfer coefficient of CO_2 at super-critical pressures in a small tube during cooling, $h(x)$, was defined as the ratio of local inner wall heat flux and local temperature deference between the CO_2 and the inner wall:

$$h(x) = \frac{q_{wall\text{-}in}(x)}{T_{CO2}(x) - T_{wall\text{-}in}(x)} \tag{1}$$

The local inner wall heat flux was calculated using an energy balance between the inner wall and the outer wall:

$$q_{wall\text{-}in}(x) = \frac{q_{wall\text{-}out}(x) \cdot d_{out}}{d_{in}} \tag{2}$$

The local outer wall heat flux, $q_{wall\text{-}out}(x)$, which was difficult to obtained through direct experimental measurement, was obtained from numerical simulations of the convection heat transfer of the cooling water in the outside annular channel formed by the plexiglass water jacket based on the measured data (inlet temperature and velocity and temperatures of the side that contacting the outer tube wall, which were assumed to equal to the outer wall temperature $T_{wall\text{-}out}(x)$) using a commercial code FLUENT 6.3. The velocity inlet and pressure outlet boundary conditions were used, with the external wall temperature distribution obtained from a 4-ordered polynomial fit of the measured $T_{wall\text{-}out}(x)$.The other side of the cooling water domain was assumed to be adiabatic. The standard k–ε model with the enhanced wall treatment was selected. The mesh was carefully designed to assure that y+ near wall is less than 1.

The inner wall temperature, $T_{wall\text{-}in}(x)$, was calculated from $T_{wall\text{-}out}(x)$ and the heat flux distribution, $q_{wall\text{-}out}(x)$, assuming one-dimensional heat conduction in the wall:

$$T_{wall\text{-}in}(x) = T_{wall\text{-}out}(x) + \frac{q_{wall\text{-}out}(x) d_{out}}{2\lambda} \ln(d_{out}/d_{in}) \tag{3}$$

The local CO_2 enthalpy, $H_{CO2}(x)$, was calculated by the inlet enthalpy which was a function of the CO_2 inlet pressure and temperature, and the integral of local heat flux (energy removed from the inlet to the local position, x) as below:

$$H_{CO2}(x) = H_{CO2}(0) - \frac{\pi d_{in}}{G_{CO2}} \int_0^x q_{wall-in}(x)dx \tag{4}$$

The local CO_2 bulk temperature, $T_{CO2}(x)$, was obtained using the NIST software REFPROP 7.0 referenced from the local CO_2 enthalpy, $H_{CO2}(x)$.

The Reynolds number based on the mean fluid temperature was defined as

$$\mathrm{Re} = \frac{\rho u d}{\mu} = \frac{4G}{\pi d \mu} \tag{5}$$

2.3. Validation of determination of the local heat flux on the tube wall

The accuracy of the local heat transfer coefficients in the vertical small tube depends on the accuracy of simulation of the convection heat transfer in the cooling water and the determination of the local outer wall heat flux, $q_{wall\text{-}out}(x)$. Therefore, the simulation of the convection heat transfer in the cooling water running through the outside channel using a commercial code FLUENT 6.3 was carefully validated experimentally.

In the validation experiments, the small tube was directly heated by electricity to produce a constant heat flux, which was calculated from the measured currents and the heater resistance, other device and measurements are similar to the experiments with CO_2. The water mass flow rate was measured by weighing method.

Physical models and numerical method was the same as described in Section 2.2.

Results showed that the general difference between numerically predicted and wall heat fluxes calculated from the heating power was about ±10%, with the maximum not exceeding 15%. Therefore, the results verify the reliable simulation for the convection heat transfer of the cooling water in the outside channel and the determination of the local outer wall heat flux of the tube.

2.4. Experimental uncertainty analysis

The uncertainty of the heat transfer coefficients was mainly caused by the heat flux predicted by numerical simulation, the wall temperature and other experimental measurement uncertainties.Prior to installation, the thermocouples and the RTDs were calibrated by the National Institute of Metrology, PR China. The accuracies were ±0.25 °C in the temperature range of 0–150 °C for the T-type thermocouples and ±0.1 °C in the temperature range of 0–70 °C for the RTDs. The accuracy of the pressure transducer

(Model EJA430A) was 0.075% of the full range of 12 MPa. According to the instructions, the accuracy of CO_2 mass flow rate measured by the Coriolis-type mass flow meter (Model MASS2100/MASS6000, MASSFLO, Danfoss) was calculated as follows:

$$\varepsilon_G = \pm\sqrt{0.1^2 + \left(\frac{Z \times 100}{m}\right)^2}$$

where ε_G = error (%), Z = zero point error (kg/h) (= 0.002 kg/h), m = mass flow (kg/h). The flow rates during the measurements were about 0.5–1.0 kg/h. Therefore, the relative uncertainties of CO_2 mass flow rates were 0.14–0.22%. Maximum uncertainty of cooling water mass flow was 0.6%.

According to the accuracies of the instruments and a detailed analysis, the uncertainty of the tube inner surface temperatures was ±0.3 °C in the temperature range of 0–150 °C, the uncertainty of the local bulk fluid temperature was ± 0.2 °C, and the relative uncertainty of the temperature difference between the wall and fluid was ±7.2%. The root-mean-square experimental uncertainty of the heat transfer coefficient was estimated to be ±16.6%. The experimental uncertainty of the inlet pressures was estimated to be ± 0.1%.

3. Experimental results and discussion

The influences of the cooling water mass flux, the CO_2 mass flux, the inlet temperature, the pressure, and the flow direction on the convection heat transfer of super-critical CO_2 inside the small tube were investigated in a series of experiments.

In cases this study concerned, the wall temperatures were lower than T_{pc}, and the bulk temperatures were higher than T_{pc} at the inlet and approached or passed T_{pc} at the outlet.

3.1. Upward flow

3.1.1. Influence of cooling water mass flux

Fig. 2 shows the effect of the cooling water mass flux on the local heat transfer coefficients for inlet conditions of T_0 = 55.0 °C, p = 8.8 MPa, $Re_{CO2,0}$ = 4340. T_{pc} = 38.9 °C at 8.8 MPa.

As shown in Fig. 2, for all these three cases, as the bulk temperature of CO_2 decreases along the test section and approaches the pseudo critical temperature, the specific heat of the CO_2 increases, which results in the enhancement of heat transfer from the CO_2 to the wall, and the local heat transfer coefficient reaches to a maximum at $x/d \approx 17$ due to the integral effect of physical properties of the fluid near the wall, especially c_p. In another respect, the density of the fluid near the wall increased dramatically due to the variation of wall temperature, and leads to the increase of turbulence due to the buoyancy effect, which is supported by the numerical simulation results in Section 5.2. These two factors combined together results in the heat transfer enhancement at $x/d \approx 17$. As is presented in Fig. 2, increasing cooling water mass flux causes a slight increase in the heat transfer coefficient for these conditions. This is due to that as the cooling water mass flow rate increases, the heat transfer between the cooling water and the external surface of the tube wall is enhanced with the increase of turbulence intensity of the cooling water, therefore the heat transfer coefficients between the CO_2 and the wall was enhanced accordingly.

3.1.2. Influence of CO_2 mass flow rate

Fig. 3 shows the effect of the CO_2 mass flow rate (corresponding to different inlet Reynolds number) on the heat transfer coefficients at $T_{CO2,0}$ = 55.0 °C, $Re_{water,0}$ = 8430, p = 8.8 MPa.

As shown in Fig. 3, the CO_2 mass flux strongly influences the heat transfer coefficient, which significantly increases as the CO_2 mass flow rate increases. When the mass flow rate is doubled, the peak of heat transfer coefficient increases by a factor of 1.5. This is mainly due to the increasing turbulence intensity with the increasing of CO_2 mass flow rate. The increased turbulence intensifies the mixing in the fluids, which enhances the heat transfer between the fluid and the wall. This is also the explanation for heat transfer coefficients increasing with the mass flow rate for constant property fluids. For CO_2 at super-critical pressures, the wall temperature increases with the mass flow rate and approaches the pseudo critical temperature stemming from the enhanced heat transfer, as a result, the specific heat of the CO_2 fluid near the wall increases accordingly, which enhances the heat transfer between the CO_2 and the wall further.

3.1.3. Influence of inlet temperature

Fig. 4 shows the heat transfer coefficients varying along the tube at $Re_{water,0}$ = 8430, $Re_{CO2,0}$ = 4340, p_0 = 8.8 MPa, with different CO_2 inlet temperatures of $T_{CO2,0}$ = 55.0 °C and 70.0 °C, respectively. When the inlet temperature is high (for case at $T_{CO2,0}$ = 70.0 °C), the specific heat and thermal conductivity of the fluid are relatively low; the heat transfer between the fluid and the wall is weak compared with that for the case with lower bulk temperature for the case with $T_{CO2,0}$ = 55.0 °C, as shown in the first part of the test section in Fig. 4. With further reduction in the bulk temperature, the difference between bulk temperatures for cases with $T_{CO2,0}$ = 55.0 °C and 70.0 °C decreases as well as that of the heat transfer coefficients.

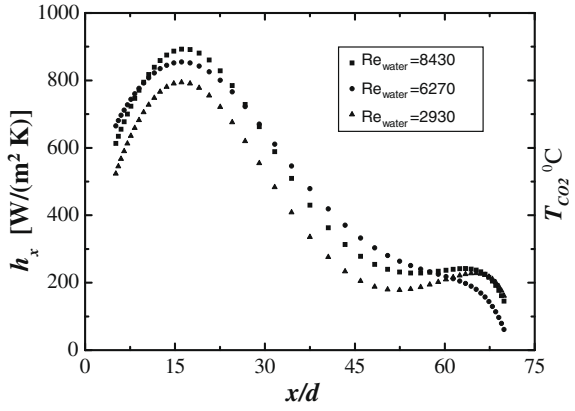

Fig. 2. Local heat transfer coefficients for various cooling water mass flow rate for upward flow d_{in} = 2.00 mm, $Re_{CO2,0}$ = 4340, p_0 = 8.8 MPa, $T_{CO2,0}$ = 55.0 °C.

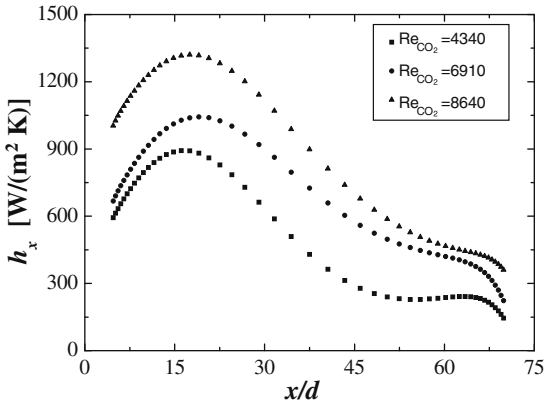

Fig. 3. Local heat transfer coefficients for various CO_2 mass flow rate for upward flow d_{in} = 2.00 mm, $Re_{water,0}$ = 8430, p_0 = 8.8 MPa, $T_{CO2,0}$ = 55.0 °C.

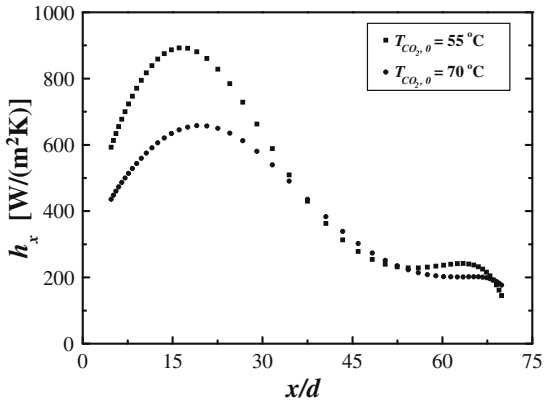

Fig. 4. Local heat transfer coefficients for various CO_2 inlet temperature for upward flow d_{in} = 2.00 mm, $Re_{water,0}$ = 8430, $Re_{CO2,0}$ = 4340, p_0 = 8.8 MPa.

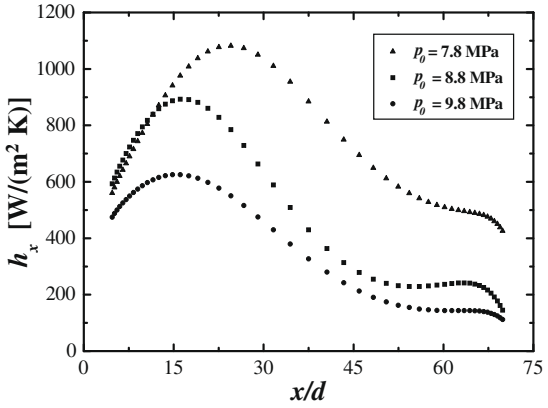

Fig. 5. Local heat transfer coefficients for various CO_2 inlet pressure for upward flow d_{in} = 2.00 mm, $Re_{water,0}$ = 8430, $Re_{CO2,0}$ = 4340, $T_{CO2,0}$ = 55.0 °C.

3.1.4. Influence of pressure

Fig. 5 shows the heat transfer coefficient of super-critical CO_2 during cooling for different pressures at $Re_{water,0}$ = 8430, $T_{CO2,0}$ = 55.0 °C, $Re_{CO2,0}$ = 4340. The heat transfer coefficient increases drastically as the pressure decreases and approaches p_c, which is mainly resulted from the increase of specific heat for cases with pressure nearer the critical pressure.

3.2. Downward flow

Heat transfer of carbon dioxide at super-critical pressures flowing downwards with inlet Reynolds number ranged from 4340 to 8640 was investigated experimentally. As shown in Figs. 6 and 7, the variation of heat transfer coefficients along the tube for downward flow cases was significantly different from the variation for upward flow cases. The heat transfer coefficients decreased first and then restored moving downstream further.

Generally, according to Jackson and Hall [24], the buoyancy parameter, Bo*, was introduced to estimate the influences of buoyancy on heat transfer for turbulent flow. The buoyancy will significantly influence the heat transfer for cases with $Bo^* > 5.6\times10^{-7}$, where Bo* was defined as:

$$Bo^* = Gr^*/(Re^{3.425}Pr^{0.8})$$

Generally, the $Gr/Re^2 > 10^{-2}$ is also a criterion for the buoyancy effect to be significant. The local value of Gr/Re^2 in cases in Figs. 6 and 7 is large than 3×10^{-1}, and the average value of Bo* is larger than 2×10^{-6}, which indicates that the buoyancy effect cannot be neglected in these cases, and buoyancy is the main factor that leads to the difference between upward flow and downward flow since other test condition are the same and flow direction is the only difference.

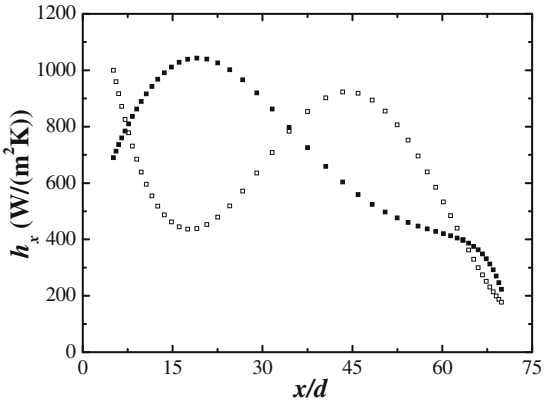

Fig. 6. Local heat transfer coefficients of CO_2 in the small tube during cooling for upward and downward flow d_{in} = 2.00 mm, $Re_{water,0}$ = 8430, $Re_{CO2,0}$ = 6910, p_0 = 8.8 MPa $T_{CO2,0}$ = 55.0 °C hollow: downward flow, solid: upward flow; $Bo^* \approx 3.1\times10^{-5}$.

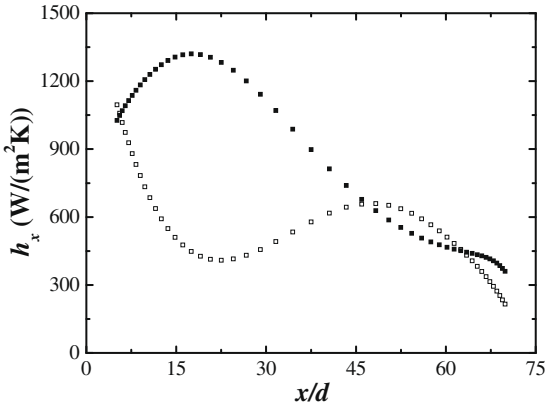

Fig. 7. Local heat transfer coefficients of CO_2 in the small tube during cooling for upward and downward flow d_{in} = 2.00 mm, $Re_{water,0}$ = 8430, $Re_{CO2,0}$ = 8640, p_0 = 8.8 Mpa $T_{CO2,0}$ = 55.0 °C hollow: downward flow, solid: upward flow; $Bo^* \approx 1.3\times10^{-5}$.

According to the theories to explain the effects of strong buoyancy on turbulence introduced by Jackson et al. [25], a sharp density change occurred when passing from a super-critical temperature (the temperature of fluid in the core) to a subcritical temperature (the wall temperature) in the cross-section, as a result, the fluid density adjacent to the wall was much larger than the density in the core. The downwards buoyancy force consists with the flow direction and accelerates the flow near the wall relatively more than in the core, the average velocity difference between the wall region and core region is reduced. Therefore, the shear stress in the region between the wall and the core was reduced since the shear stress was proportional to the average velocity difference between these two regions. As a result, the production of turbulence was reduced due to the flattened velocity profile and the heat transfer coefficients were reduced as well. Moving downstream along the tube, the buoyancy force enhanced the negative shear stresses, thus restored the production of turbulence, and improved the heat transfer again. For certain case during cooling, such as in Fig. 6, the local heat transfer coefficient for downward flow was even larger than that at upward flow conditions in the downstream of the test section where the heat transfer

recovered. This is mainly due to that the bulk temperature and wall temperature for downward flow was slightly higher than for upward flow resulted from the impaired heat transfer in the first part of the test section, and the heat transfer was recovered more in the downstream, which was different from the cases during heating.

4. Physical–mathematical model

The physical model and coordinate system for the numerical analysis are shown in Fig. 8. The complete computational domain covered the CO_2 fluid, the tube wall and the cooling water. The length of the cooled section is 150 mm, and the length of the sections before and after the cooled section are assumed to be 50 mm ($25d$). Flow enters the tube with a constant velocity, u_0, and constant temperature, T_0. The flow was assumed to be axial-symmetric, steady, and turbulent flow.

In this study, the conjugate heat transfer of water–solid wall–CO_2 in a counter-flow heat exchanger was numerically simulated using a commercial code FLUENT 6.3 with various turbulence models used to model the turbulence, including the RNG k–ε model with the two-layer approach [26] and three low-Reynolds number models: Yang and Shih (YS) [27], Abe et al. (AKN) [28], and Lam and Bremhorst (LB) [29].

The governing equations for the steady state, axial-symmetric turbulent flow of a super-critical pressure fluid in a vertical tube with consideration of the temperature-dependent property variations and buoyancy described by He [30] was employed.

The definitions of damping functions, f_1, f_2 and f_μ in low-Reynolds number turbulence models can be found in details in [27–29].

The NIST Standard Reference Database 23 (REFPROP) Version 7 was used for calculating the temperature and pressure dependent properties of CO_2. The SIMPLEC algorithm was used to couple the pressure and velocities. The second-order upwind scheme was used for discretization of the momentum, energy, turbulent kinetic energy, and turbulent energy dissipation equations. The structured mesh with 250 nodes in axial direction, (60 + 20) nodes in radius direction (CO_2 region + tube wall), 150 nodes in axial direction and 60 nodes in radius direction for cooling water region was used. The mesh was refined in the radial direction towards the tube wall for both carbon dioxide and water region and was carefully designed to assure that the y+ value at the first node was always less than 1. Boundary conditions imposed were uniform velocity and temperature at the inlet, and pressure outlet conditions at the outlet for both CO_2 region and cooling water region. The convergence criteria required a decrease of at least 6 orders of magnitude for the residuals with no observable change in the surface temperatures for an additional 200 iterations. Calculations with various numbers of elements showed that the results were grid independent.

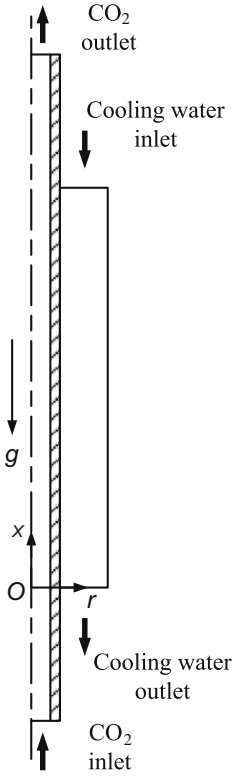

Fig. 8. Physical model and coordinate system for numerical simulation (for upward flow, g is reversed for downward flow).

5. Numerical simulation results and analysis

5.1. Comparison of calculated results of different turbulence models and experimental data of the wall temperature

Fig. 9 compares the measured and the predicted wall temperatures for super-critical pressure CO_2 flowing upwards in the vertical small tube during cooling for $Re_{CO2,0}$ = 4216, $Re_{water,0}$ = 8430, p_0 = 8.8 MPa, $T_{CO2,0}$ = 70.0 °C using various turbulence models including the RNG k–ε model with the two-layer approach and three low-Reynolds number models: YS, AKN, and LB. The experimental data show that the wall temperature increases close to the entrance and then decreases monotonically. The simulations show that the RNG k–ε turbulence model predicted the best quantitatively corresponding wall temperature after the wall temperature peak. However, the RNG k–ε turbulence model overestimates the of heat transfer near the cooling entrance. Although the low-Reynolds number models: AKN, LB and YS model seriously over-predicted the wall temperature, they were able to reproduce the general trend, especially the enhancement of heat transfer close to the entrance. The YS model predicts a clearer occurrence of heat transfer enhancement and a closer wall temperature compared with the AKN and LB model.

Fig. 10 compares the measured and the predicted wall temperatures for super-critical pressure CO_2 for both upward and downward flow in the vertical small tube during cooling for $Re_{CO2,0}$ = 4340, $Re_{water,0}$ = 8340, p_0 = 8.8 MPa, $T_{CO2,0}$ = 55.0 °C using the RNG k–ε model with the two-layer approach and the YS model. The experimental data for downward flow clearly show deterioration and recovery of heat transfer due to the buoyancy effect. The RNG k–ε model responds weakly to the buoyancy effects for downward flow. The YS model shows a strong response to the buoyancy

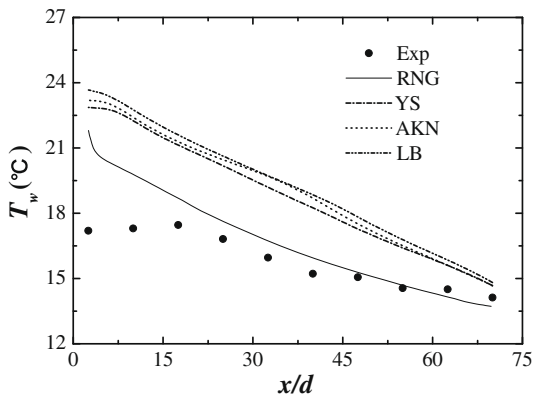

Fig. 9. comparison for upward flow: various turbulence model $Re_{CO2,0}$ = 4216, $Re_{water,0}$ = 8430, p_0 = 8.8 MPa, $T_{CO2,0}$ = 70.0 °C.

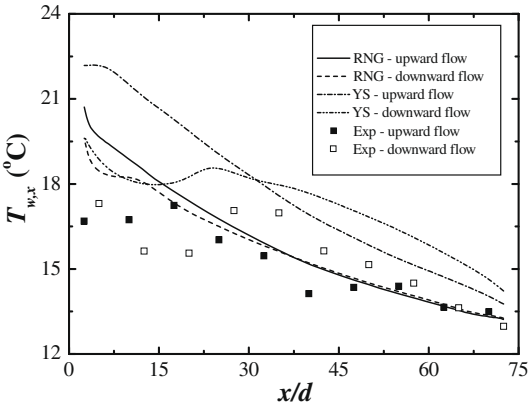

Fig. 10. Comparison for upward and downward flow using various turbulence model $Re_{CO2,0}$ = 4340, $Re_{water,0}$ = 8430, p_0 = 8.8 MPa, $T_{CO2,0}$ = 55.0 °C.

and is able to predict the occurrence of deterioration and recovery exhibited in the experiments. Therefore, the following analyses were based on the detailed information generated by the numerical simulations using the YS model.

5.2. Analysis of heat transfer mechanism for upward flow

For CO_2 at super-critical pressures flowing upwards in the vertical small tube during cooling, a peak value of heat transfer coefficients occurs as shown in Figs. 2–5. However, the peak in the heat transfer coefficient does not occur at the position where bulk temperature equals to T_{pc}, which means that the peak in the heat transfer coefficient and that of the specific heat do not coincide exactly. This is different from those found for the axially-averaged heat transfer coefficients as reported in previous research, such as [12,13]. Fig. 11 depicts the variation of kinetic energy along the tube within the fluid layer adjacent to the wall where $y+ < 60$ for $Re_{CO2,0}$ = 4216, $Re_{water,0}$ = 8430, p_0 = 8.8 MPa, $T_{CO2,0}$ = 70.0 °C. A peak value of turbulent kinetic energy occurs near the entrance due to the sharp variation of density (which can be verified in Section 5.3) as well as the buoyancy effect, where the wall temperature decreases dramatically from the value equals to bulk temperature in the adiabatic flow inlet part. As a result, the fluid density near the wall increases sharply, whereas the core of the fluid still stays in the gaseous state and the density is very low. The sharp variation of the density from the core to the near wall increases the turbulent kinetic energy and the mixing of fluids, and therefore enhanced the heat transfer between the fluid and the wall. The direction of buoyancy force induced by this sharp density change is opposite to the flow direction for upward flow, which also enhances the heat transfer.

Moving further downstream, the bulk temperature decreases and the temperature of the fluid layer adjacent to the wall decreases as well and approaches T_{pc}, a peak value of specific heat occurs, which increases the heat diffusivity, and the heat transfer is enhanced as a result.

The combination influence of turbulent kinetic energy and specific heat in the fluid layer adjacent to the wall other than the bulk properties leads to the variation of heat transfer coefficients along the tube.

5.3. Effects of thermophysical properties

Fig. 12 presents the influence of thermophysical properties including density, specific heat, viscosity and thermal conductivity on wall temperature for $Re_{CO2,0}$ = 4216, $Re_{water,0}$ = 8430, p_0 = 8.8 MPa, $T_{CO2,0}$ = 70.0 °C. In the calculations two different cases were considered: (1) all of the thermophysical properties are variable; and (2) only one thermophysical property was held constant based on the inlet fluid temperature to study the influence of each physical property, respectively.

It can be seen that for such conditions with low inlet Reynolds number and strong buoyancy effect, the influence of fluid density is significant. The turbulent kinetic energy is greatly reduced when the density is held constant and the peak disappears as shown in Fig. 13. As a result, the wall temperature in this position is much lower than the temperature-dependent density case, which indicates a poorer heat transfer, and the enhancement near the entrance disappears as well without the buoyancy effect. The specific heat also significantly influences heat transfer. The heat transfer is weakened when the specific heat is held constant at inlet temperature which is far from T_{pc}.

5.4. Heat transfer enhancement and deterioration mechanism due to buoyancy effects

Heat transfer enhancement for upward flow (buoyancy-opposed) and deterioration and recovery for downward (buoyancy-assisted) flow due to buoyancy were observed in cases this study concerned, and the YS model was able to reproduce the general trend of wall temperature distribution exhibited in the experiments, as shown in Fig. 10.

The buoyancy effect induced by gravity and density variation plays a significant role for both upward and downward flow. The fluid changes from a gas-like state in the core to a liquid-like state near the wall. For both upward and downward flow, the velocity decreases along the tube due to the increase of density dependent on fluid temperature. For upward flow, the direction of buoyancy force is opposite to the flow direction, the buoyancy force accelerates the flow near the wall relatively more than in the core, the velocity profiles are steeper that those when $g = 0$ (as shown in Fig. 14), as a result, the shear stress is intensified and thus, more turbulence is generated and diffused, and turbu-

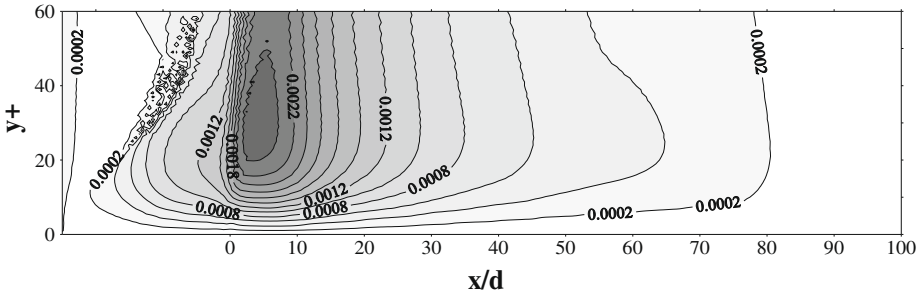

Fig. 11. Variation of kinetic energy along the tube for upward flow $Re_{CO2,0}$ = 4216, $Re_{water,0}$ = 8430, p_0 = 8.8 MPa, T_{in} = 70.0 °C.

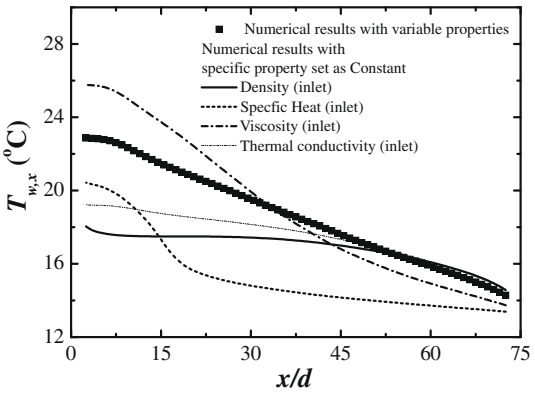

Fig. 12. Influence of thermophysical properties on the wall temperatures $Re_{CO2,0}$ = 4216, $Re_{water,0}$ = 8430, p_0 = 8.8 MPa, T_{in} = 70.0 °C upward flow.

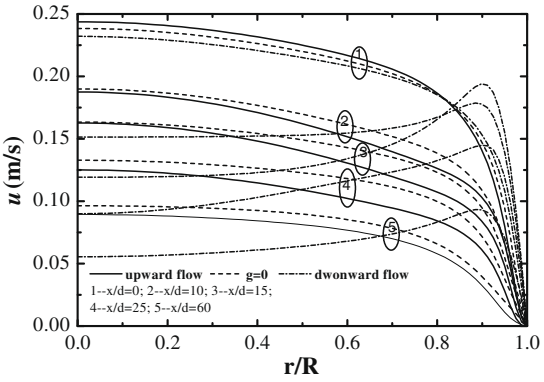

Fig. 14. Influence of buoyancy on velocity profiles $Re_{CO2,0}$ = 4340, $Re_{water,0}$ = 8430, p_0 = 8.8 MPa, $T_{CO2,0}$ = 55.0 °C.

lent kinetic energy is increased accordingly compared with the buoyancy free case.

For downward flow cases when the direction of buoyancy force consists with the flow direction, the velocity profiles are flattened and the turbulent kinetic energy reduced greatly, as shown in Figs. 14 and 15, x/d = 10 and x/d = 15 where the heat transfer was impaired as the consequence of the buoyancy effect. Moving downstream along the tube, the M-shaped velocity profile increases the negative shear stress, and partially restored the turbulent kinetic energy, as shown in Figs. 14 and 15, at x/d = 25, where the heat transfer was improved.

6. Conclusions

The local heat transfer coefficients of CO_2 at super-critical pressures in vertical small tubes during cooling were determined by combining simulations of the convection heat transfer in the cooling water in the outside channel with experimental measurements.

The effects of the cooling water mass flow rate, the CO_2 mass flow rate, the CO_2 inlet temperature, the operating pressure and the flow direction were analysed. The heat transfer coefficients increase with increasing cooling water mass flow rate, increase significantly with increasing CO_2 mass flow rate, and decrease with the operating pressure for pressures above p_c. The heat transfer

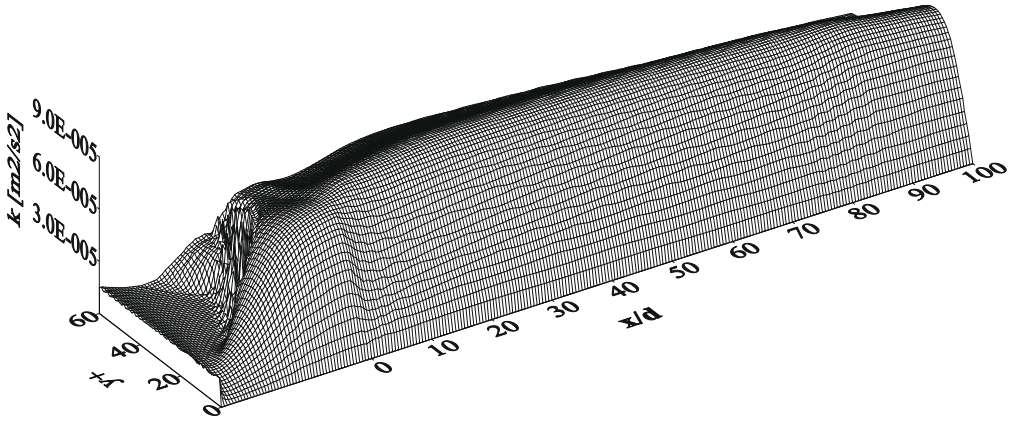

a) Density is held constant

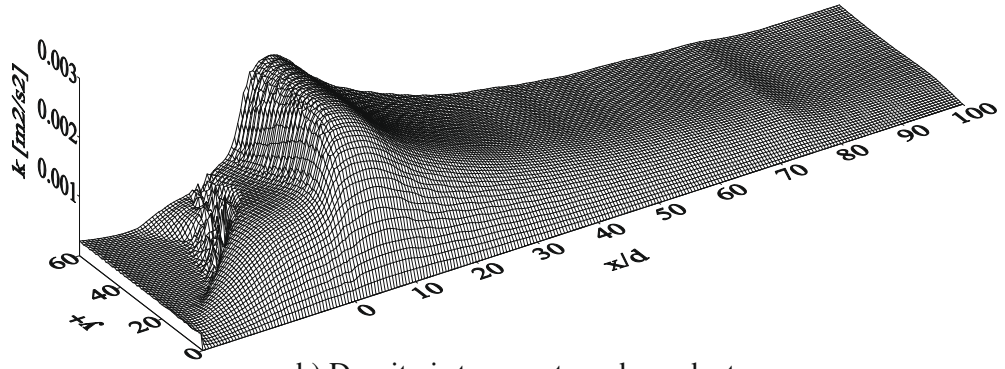

b) Density is temperature-dependent

Fig. 13. Influence of density on turbulent kinetic energy $Re_{CO2,in}$ = 4216, $Re_{cw,in}$ = 8430, p_0 = 8.8 MPa, T_{in} = 70.0 °C upward flow.

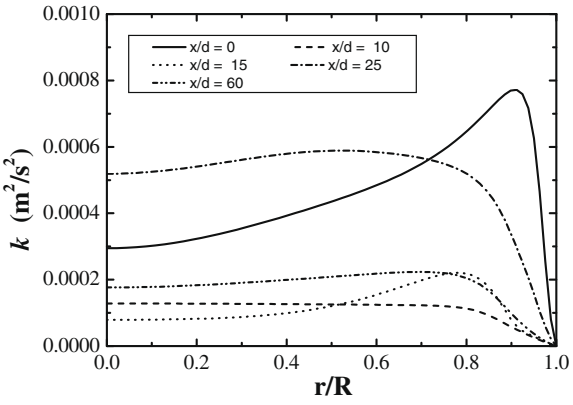

Fig. 15. Turbulent kinetic energy distribution at different axial location for downward flow$Re_{CO2,0}$ = 4340, $Re_{water,0}$ = 8430, p_0 = 8.8 MPa, $T_{CO2,0}$ = 55.0 °C.

was enhanced for upward flow and impaired for downward flow due to buoyancy effect when the inlet Reynolds number was relatively small.

The local heat transfer coefficients of CO_2 varied along the small tube for both upward flow and downward flow. For upward flow, the heat transfer coefficients firstly increased and then decreased with a maximum occurring between the position of the peak of turbulent kinetic energy and the peak of specific heat in the layer adjacent to the wall. For downward flow, the heat transfer coefficients firstly decreased due to the buoyancy effect and then increased when the heat transfer improved, and decreased again after reaching maximum near the recovery position of turbulent kinetic energy.

The simulations using the low-Reynolds number k–ε turbulence model due to Yang–Shih has been found to be able to reproduce the general features exhibited in the experiments on convection heat transfer to CO_2 at super-critical pressures in a vertical small tube during cooling, especially the enhancement and deterioration due to buoyancy effects, although with a relatively large overestimation of measured wall temperatures. The RNG k–ε turbulence model responds weakly to the buoyancy effects.

A better understanding of the problem has been developed based on the information generated by the simulations using the Yang–Shih model: the turbulence kinetic energy and specific heat of fluids adjacent to the wall play a very important role in the convection heat transfer to CO_2 at super-critical pressures in a vertical small tube during cooling; for small tubes such as the one used in the current study, the buoyancy effect is generally significant when the CO_2 inlet Reynolds number is relatively small (less than 10^4); the sharp variations of density and specific heat dependent on temperature greatly affect the heat transfer to CO_2 at super-critical pressures in a vertical small tube during cooling.

Acknowledgments

This project was supported by a Key Grant Project of the Chinese Ministry of Education (No. 306001) and the National High Technology Research and Development Program of China (863 Program) (No. 2006AA05Z416). We thank Professor J.D. Jackson in the School of Mechanical, Aerospace and Civil Engineering, the University of Manchester, UK, and Dr. S. He in the School of Engineering, University of Aberdeen, UK, for their many suggestions for this research. We also thank Prof. David Christopher for editing the English.

References

[1] G. Lorentzen, J. Pettersen, A new efficient and environmentally benign system for car air-conditioning, Int. J. Refrig. 16 (1) (1993) 4–12.
[2] S.B. Riffat, C.F. Afonso, A.C. Oliveria, Natural refrigerants for refrigeration and air-conditioning systems, Appl. Therm. Eng. 17 (1) (1997) 33–42.
[3] B.S. Petukhov, Heat transfer and friction in turbulent pipe flow with variable physical properties, Adv. Heat Transfer 6 (1970).
[4] W.B. Hall, Heat transfer near the critical point, Adv. Heat Transfer 7 (1971).
[5] J.D. Jackson, W.B. Hall, J. Fewster, A. Watson, M.J. Watts, Heat transfer to supercritical pressure fluids, U.K.A.E.A. A.E.R.E.-R 8158, Design Report 34, 1975.
[6] P.X. Jiang, Y. Zhang, R.F. Shi, Experimental and numerical investigation of convection heat transfer of CO_2 at super-critical pressures in a vertical mini tube, Int. J. Heat Mass Transfer 51 (11–12) (2008) 3052–3056.
[7] P.X. Jiang, Y. Zhang, Y.J. Xu, R.F. Shi, Experimental and numerical investigation of convection heat transfer of CO_2 at super-critical pressures in a vertical tube at low Reynolds numbers, Int. J. Therm. Sci. 47 (8) (2008) 3052–3056.
[8] M. Sharabi, W. Ambrosini, Prediction of turbulent convection heat transfer to a fluid at super-critical pressure in square and triangular channels, Ann. Nucl. Energy 35 (2008) 993–1005.
[9] E.A. Krasnoshchekov, V.S. Protopopov, Experimental study of heat exchange in carbon dioxide in the super-critical range at high temperature drops, Teplofizika Vysokikh Temperature 4 (3) (1966) 389–398 (in Russian).
[10] V.L. Baskov, I.V. Kuraeva, V.S. Protopopov, Heat transfer with the turbulent flow of a liquid at super-critical pressure in tube under cooling condition, Teplofizika Vysokikh Temperature 15 (1) (1977) 96–102.
[11] S.H. Yoon, J.H. Kim, Y.W. Hwang, M.S. Kim, K. Min, Y. Kim, Heat transfer and pressure drop characteristics during the in-tube cooling process of carbon dioxide in the super-critical region, Int. J. Refrig. 26 (2003) 857–864.
[12] C.H. Son, S.J. Park, An experimental study on heat transfer and pressure drop characteristics of carbon dioxide during gas cooling process in a horizontal tube, Int. J. Refrig. 29 (4) (2006) 539–546.
[13] J. Pettersen, R. Rieberer, A. Leister, Heat transfer and pressure drop characteristics of super-critical carbon dioxide in microchannel tubes under cooling, in: Proceedings of Fourth IIR-Gustav Lorentzen Conference on Natural Working Fluids in Purdue, Joint Conference of the International Institute of Refrigeration, Sections B and E, 1998, pp. 99–106.
[14] S.M. Liao, T.S. Zhao, An experimental investigation of convection heat transfer to super-critical carbon dioxide in miniature tubes, Int. J. Heat Mass Transfer 45 (25) (2002) 5025–5034.
[15] C.B. Dang, E. Hihara, In-tube cooling of super-critical carbon dioxide. Part 1. Experimental measurement, Int. J. Refrig. 27 (2004) 736–747.
[16] X.L. Huai, S. Koyama, T.S. Zhao, An experimental study of flow and heat transfer of super-critical carbon dioxide in multi-port mini channels under cooling conditions, Chem. Eng. Sci. 60 (2005) 3337–3345.
[17] G.H. Kuang, M. Ohadi, Semi-empirical correlation of gas cooling heat transfer of super-critical carbon dioxide in micro channels, Int. J. HVAC&R Res. 14 (6) (2008) 861–870.
[18] S.S. Pitla, D.M. Robinson, E.A. Groll, S. Ramadhyani, Heat transfer from supercritical carbon dioxide in tube flow: a critical review, Int. J. HVAC&R Res. 4 (3) (1998) 281–301.
[19] L.X. Chen, G. Ribatskia, J.R. Thome, Analysis of supercritical CO_2 cooling in macro- and micro-channels, Int. J. Refrig. 31 (2008) 1301–1316.
[20] S.M. Liao, T.S. Zhao, A numerical investigation of laminar convection of supercritical carbon dioxide in vertical mini/micro tubes, Prog. Comput. Fluid Dyn. 2 (2/3/4) (2002) 144–152.
[21] N.E. Petrov, V.N. Popov, Heat transfer and resistance of carbon dioxide being cooled in super-critical region, Therm. Eng. 32 (3) (1985) 131–134.
[22] S.S. Pitla, S. Ramadhyani, E.A. Groll, Convective heat transfer from in-tube flow of turbulent super-critical carbon dioxide. Part 1. Numerical analysis, Int. J. HVAC&R Res. 7 (4) (2001) 345–366.
[23] C.B. Dang, E. Hihara, In-tube cooling of super-critical carbon dioxide. Part 2. Comparison of numerical calculation with different turbulence models, Int. J. Refrig. 27 (2004) 748–760.
[24] J.D. Jackson, W.B. Hall, Influences of buoyancy on heat transfer to fluids flowing in vertical tubes under turbulent conditions, in: S. Kakac, D.B. Spalding (Eds.), Turbulent Forced Convection in Channels and Bundles, vol. 2, Hemisphere, New York, 1979, pp. 613–640.
[25] J.D. Jackson, M.A. Cotton, B.P. Axcell, Study of mixed convection in vertical tubes, Int. J. Heat Fluid Flow 10 (1989) 2–15.
[26] V. Yakhot, S.A. Orszag, Renormalization group analysis of turbulence: I. Basic theory, J. Sci. Comput. 1 (1) (1986) 1–51.
[27] Z. Yang, T.H. Shih, New time scale based k–ε model for near wall turbulence, AIAA J. 31 (1993) 1191–1198.
[28] K. Abe, T. Kondoh, Y. Nagano, A new turbulence model for predicting fluid flow and heat transfer in separating and reattaching flows – I Flow field calculations, International Journal of Heat and Mass Transfer 37 (1994) 139–151.
[29] C.K.G. Lam, K.A. Bremhorst, Modified form of k–ε model for predicting wall turbulence ASME, J. Fluids Eng. 103 (1981) 456–460.
[30] S. He, W.S. Kim, P.X. Jiang, J.D. Jackson, Simulation of mixed convective heat transfer to carbon dioxide at supercritical pressure, J. Mech. Eng. Sci. 218 (2004) 1281–1296.